JOURNAL OF VIROLOGY, May 2011, p. 4679–4690 Vol. 85, No. 10
0022-538X/11/$12.00 doi:10.1128/JVI.02456-10

Role of Nrf2 in Host Defense against Influenza Virus in Cigarette Smoke-Exposed Mice▽

Yuichi Yageta,[1] Yukio Ishii,[1]* Yuko Morishima,[1] Hironori Masuko,[1] Satoshi Ano,[1] Tadahiro Yamadori,[1] Ken Itoh,[2] Kaoru Takeuchi,[3] Masayuki Yamamoto,[4] and Nobuyuki Hizawa[1]

Department of Respiratory Medicine,[1] and Department of Infectious Biology,[3] University of Tsukuba, Tsukuba, Japan; Center for Advanced Medical Research, Hirosaki University School of Medicine, Hirosaki, Japan[2]; and Department of Medical Biochemistry, Tohoku University Graduate School of Medicine, Sendai, Japan[4]

Received 24 November 2010/Accepted 24 February 2011

Influenza virus is a common respiratory tract viral infection. Although influenza can be fatal in patients with chronic pulmonary diseases such as chronic obstructive pulmonary disease, its pathogenesis is not fully understood. The Nrf2-mediated antioxidant system is essential to protect the lungs from oxidative injury and inflammation. In the present study, we investigated the role of Nrf2 in protection against influenza virus-induced pulmonary inflammation after cigarette smoke exposure with both *in vitro* and *in vivo* approaches. For *in vitro* analyses, peritoneal macrophages isolated from wild-type and *Nrf2*-deficient mice were treated with poly(I:C) and/or cigarette smoke extract. For *in vivo* analysis, these mice were infected with influenza A virus with or without exposure to cigarette smoke. In *Nrf2*-deficient macrophages, NF-κB activation and the induction of its target inflammatory genes were enhanced after costimulation with cigarette smoke extract and poly(I:C) compared with wild-type macrophages. The induction of antioxidant genes was observed for the lungs of wild-type mice but not those of *Nrf2*-deficient mice after cigarette smoke exposure. Cigarette smoke-exposed *Nrf2*-deficient mice showed higher rates of mortality than did wild-type mice after influenza virus infection, with enhanced peribronchial inflammation, lung permeability damage, and mucus hypersecretion. Lung oxidant levels and NF-κB-mediated inflammatory gene expression in the lungs were also enhanced in *Nrf2*-deficient mice. Our data indicate that the antioxidant pathway controlled by Nrf2 is pivotal for protection against the development of influenza virus-induced pulmonary inflammation and injury under oxidative conditions.

Influenza virus (FluV), including types A, B, and C, is a ubiquitous airway pathogen especially prevalent in the winter season. Type A FluV is the most virulent human pathogen of the three and sometimes gives rise to human influenza pandemics, such as the 2009 swine-origin flu (6). FluV infection is associated with exacerbations of various pulmonary diseases, particularly acute exacerbations in chronic obstructive pulmonary disease (COPD) (12, 38). Recent studies have demonstrated that the severity of infection in patients with COPD depends on both viral and host factors (24).

FluV infection induces several host immune and inflammatory responses via Toll-like receptor 3 (TLR3), which is expressed on myeloid dendritic cells, macrophages, and respiratory epithelial cells and recognizes viral double-stranded RNA (dsRNA) (39). In response to dsRNA stimulation, TLR3 recruits its adaptor protein TRIF, which indirectly activates the transcription factors interferon regulatory factor 3 (IRF-3) and nuclear factor κB (NF-κB) (19). IRF-3 then induces the expression of beta interferon (IFN-β), while NF-κB induces the genes that encode inflammatory cytokines such as tumor necrosis factor alpha (TNF-α) and CXC chemokines such as interleukin-8 (IL-8), macrophage inflammatory protein 2 (MIP-2), and keratinocyte-derived chemokine (KC). NF-κB has been described to be a redox-sensitive transcription factor, and it can be activated by reactive oxygen species (ROS) (26). These findings suggest that the costimulation of macrophages with TLR3 ligands and ROS would enhance the activation of NF-κB.

It was demonstrated previously that cigarette smoke (CS), which contains a variety of oxidants, activates NF-κB, particularly in macrophages (40). The level of nuclear translocation of NF-κB was significantly higher in the lungs of healthy smokers and current smokers with COPD than in ex-smokers with COPD, suggesting that NF-κB activation is most influenced by current smoking status (33). Smoking cessation was demonstrated previously to reduce the risk of COPD exacerbation (3). These findings indicate that FluV infection under oxidative conditions induced by smoke exposure strongly enhances pulmonary inflammation by the activation of NF-κB, followed by the induction of proinflammatory gene expression. It is also possible that the antioxidant capacity of the host might be a critical factor in regulating susceptibility to COPD exacerbation after FluV infection.

Mammalian cells produce several antioxidant enzymes and defense proteins against environmental and oxidative stimuli. The transactivation of the majority of antioxidant and defense genes is regulated by Nrf2 through binding to antioxidant response elements (AREs) on their 5′ promoters. Nrf2 is a member of the family of cap'n'collar basic leucine zipper transcription factors expressed abundantly in macrophages (17). A

* Corresponding author. Mailing address: Institute of Clinical Medicine, University of Tsukuba, 1-1-1 Tennoudai, Tsukuba, Ibaraki 305, Japan. Phone and fax: 81-298-53-3144. E-mail: ishii-y@md.tsukuba.ac.jp.

▽ Published ahead of print on 2 March 2011.

protective role of Nrf2 was demonstrated previously with animal models of oxidant-related pulmonary disorders such as emphysema (16, 28), acute lung injury (10, 29), and pulmonary fibrosis (9, 21).

Therefore, we hypothesized that Nrf2 is a critical factor that protects against the development of pulmonary inflammation induced by FluV under oxidative conditions. We first investigated the effects of Nrf2 on the activation of NF-κB after stimulation with both TLR3 ligands and cigarette smoke extract (CSE) using a macrophage culture system. We then investigated the role of Nrf2 in protection against the FluV-induced exacerbation of pulmonary inflammation during CS exposure using Nrf2-deficient ($Nrf2^{-/-}$) mice.

MATERIALS AND METHODS

Animals. C57BL/6 wild-type (WT) mice were purchased from SLC Japan (Shizuoka, Japan). $Nrf2^{-/-}$ mice were generated as described previously (18). Mice at 7 to 9 weeks of age were divided into three groups: the control group, with clean air and saline inoculation; the FluV group, with clean air and intranasal inoculation with 250 PFU of FluV (A/PR/8/34) in 50 μl saline; and the CS-plus-FluV group, which was exposed to 10 cigarettes (Hi-lite; Japan Tobacco Inc., Tokyo, Japan) daily for 4 consecutive days and inoculated with 250 PFU FluV after 4 days. All animal studies were approved by the Institutional Review Board of the University of Tsukuba.

CSE. Cigarette smoke extract (CSE) was prepared by bubbling smoke from one cigarette into 10 ml of RPMI 1640 medium at a rate of 1 cigarette per 2 min as described previously (41). CSE was standardized by measuring the absorbance at 320 nm. The pH of the CSE was adjusted to 7.3 to 7.5, and the CSE was then passed through a 0.2-μm filter for sterilization. The prepared CSE was defined as 100% CSE and was diluted with serum-free RPMI 1640 medium before use.

Macrophages. Peritoneal macrophages were elicited by the intraperitoneal injection of thioglycolate as described previously (5). Macrophages were cultured at 3×10^5 cells/ml in a 24-well plate with CSE, poly (I:C) (Sigma-Aldrich, St. Louis, MO), or both.

Bronchoalveolar lavage (BAL). The lungs were lavaged with six sequential 1-ml aliquots of saline. The first set of lavage fluid was used for protein assays or enzyme-linked immunosorbent assays (ELISAs). Total cells were counted with a hemocytometer, and differential cell counts were obtained after staining with Diff-Quik.

Real-time RT-PCR. Total RNA was extracted from peritoneal macrophages or whole lung tissues, and real-time quantitative reverse transcription (RT)-PCR was performed by using a sequence detector (ABI7700; Applied Biosystems, Foster City, CA). PCR primers for TNF-α, KC, MIP-2, IFN-β, NAD(P)H-quinone oxidoreductase 1 (NQO1), the heavy subunit of gamma glutamyl cysteine synthetase (GCLC), the light subunit of gamma glutamyl cysteine synthetase (GCLM), heme oxygenase 1 (HO-1), and influenza A virus nucleoprotein (NP) are listed in Table 1. Target gene expression was normalized to glyceraldehyde-3-phosphate dehydrogenase (GAPDH) gene expression.

Western blotting. Nuclear extracts of peritoneal macrophages or whole lungs were made by using a nuclear extraction kit (Panomics, Redwood City, CA) according to the manufacturer's instruction. Ten to twenty micrograms of nuclear extracts was separated with 10% SDS-PAGE gels and transferred onto polyvinylidene difluoride (PVDF) membranes. After the blocking of nonspecific sites, the PVDF membranes were incubated with anti-NF-κB p65, anti-IRF-3, and anti-Nrf2 rabbit polyclonal antibodies (1:500; Santa Cruz Biotechnology, Santa Cruz, CA), followed by incubation with horseradish peroxidase-conjugated secondary antibody. Specific bands were visualized with enhanced chemiluminescence reagent (GE Healthcare, Buckinghamshire, England) and exposed to X-ray film. Lamin B was used as an internal control.

Protein assay. The protein level in the BAL fluids, an indicator of lung permeability damage, was determined by using a DC protein assay kit (Bio-Rad Laboratories, Hercules, CA).

ELISA. The concentrations of TNF-α and KC in the first BAL fluids and lung homogenates were determined by an ELISA (R&D Systems, Minneapolis, MN) according to the manufacturer's protocol. The concentration of the MUC5AC protein in the first BAL fluid sample was measured by an ELISA, as previously described (34). Briefly, 50 μl of each sample was added to a Costar EIA/RIA plate (Corning Glass, Corning, NY) and dried overnight at 40°C. After blocking with 2% bovine serum albumin (fraction V; Sigma), the plate was incubated with a mouse monoclonal antibody to MUC5AC (1:200, clone 45M1; Thermo Fisher Scientific, Fremont, CA). After incubation with a horseradish peroxidase-conjugated goat anti-mouse IgG, the plate was developed with 3,3′,5,5′-tetramethylbenzidine (TMB) solution (Wako Pure Chemical Industries, Osaka, Japan), and the reaction was stopped with 1 M sulfuric acid. The absorbance was measured at 450 nm by using a spectrophotometer.

TABLE 1. Primers used for RT-PCR

Primer target	Sequence
TNF-α	5′-CCCTCACACTCAGATCATCTTCT-3′
	5′-GCTACGACGTGGGCTACAG-3′
MIP-2	5′-ACTCTCAAGGGCGGTCAAAA-3′
	5′-TTCCAGGTCAGTTAGCCTTGC-3′
KC	5′-AGACCATGGCTGGGATTCAC-3′
	5′-TGAACCAAGGGAGCTTCAGG-3′
IFN-β	5′-ACCTACAGGGCGGACTTCAA-3′
	5′-TCTGGAGCATCTCTTGGATGG-3′
NQO1	5′-AGCCAATCAGCGTTCGGTA-3′
	5′-GAATGGGCCAGTACAATCAGG-3′
GCLC	5′-GCACATCTACCACGCAGTCA-3′
	5′-GAACATCGCCTCCATTCAGT-3′
GCLM	5′-ACCGGGAACCTGCTCAACT-3′
	5′-GCTGATTTGGGAACTCCATT-3′
HO-1	5′-GAATGAACACTCTGGAGATGACAC-3′
	5′-TGTGAGGGACTCTGGTCTTTG-3′
GAPDH	5′-TGTGTCCGTCGTGGATCTGA-3′
	5′-CCTGCTTCACCACCTTCTTGAT-3′
NP	5′-GACGATGCAACGGCTGGTCTG-3′
	5′-AGCATTGTTCCAACTCCTTT-3′

Histopathology and immunohistochemistry. The lungs were fixed with 10% neutral buffered formalin with 25 cm of H_2O pressure and embedded in paraffin. For histopathology, 2-μm-thick sections were stained with hematoxylin and eosin for pathological evaluation and periodic acid-Schiff (PAS) reagent to identify neutral mucosubstances. For immunohistochemistry, 4-μm-thick sections were immunostained with the above-mentioned anti-Nrf2 polyclonal antibody (1:200) or anti-8-hydroxy-deoxyguanosine (8-OHdG) monoclonal antibody (1 μg/ml; Japan Institute for the Control of Aging, Shizuoka, Japan) after incubation with 3% hydrogen peroxide to inhibit endogenous peroxidase activity. The sections were developed by using a Histofine mouse stain kit (Nichirei Biosciences, Tokyo, Japan) and a diaminobenzidine (DAB) solution according to the manufacturer's instructions. Finally, the sections were counterstained with methyl green or hematoxylin.

Lung water content. The whole-lung weight was measured before and after drying at 80°C for 48 h to calculate ratios.

Statistics. Data are expressed as the means ± standard errors of the means (SEM). Multiple comparisons were performed by using one-way analysis of variance (ANOVA) and a *post hoc* Student-Newman-Kuels test. Body weight and viral load data were analyzed by two-way ANOVA and a *post hoc* Student-Newman-Kuels test. Survival data were analyzed by the Kaplan-Meier method and log rank test. P values of <0.05 were considered to be statistically significant.

RESULTS

Effects of Nrf2 on the induction of immune- and inflammatory-related genes in macrophages. The innate immune system is the primary defense mechanism against infectious pathogens. Macrophages play an important role in the regulation of immune and inflammatory responses against environmental stimuli such as viral infections and CS. We initially assessed the

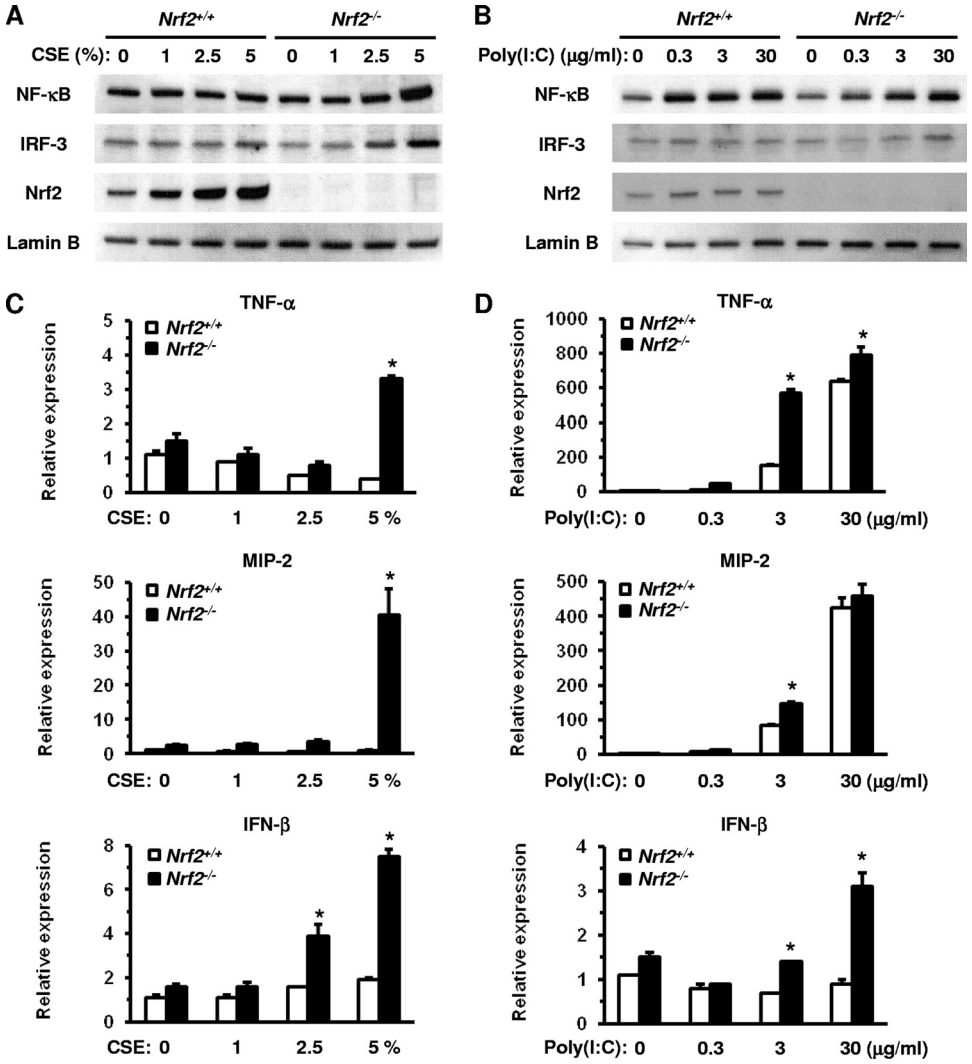

FIG. 1. Activation of transcription factors and induction of their target cytokine/chemokine genes in peritoneal macrophages after stimulation with the indicated levels of cigarette smoke extract (CSE) or poly(I:C). (A and B) Nuclear translocation of the transcription factors NF-κB, IRF-3, and Nrf2 in peritoneal macrophages of wild-type ($Nrf2^{+/+}$) mice and Nrf2-deficient ($Nrf2^{-/-}$) mice 6 h after exposure to CSE (A) or poly(I:C) (B). Lamin B was used as an internal control. (C and D) mRNA expression of TNF-α (top), MIP-2 (middle), and IFN-β (bottom) in peritoneal macrophages of $Nrf2^{+/+}$ and $Nrf2^{-/-}$ mice 24 h after exposure to CSE (C) or poly(I:C) (D). Each expression was normalized against GAPDH mRNA. Data are expressed as the means ± SEM ($n = 3$). ∗, significant difference between $Nrf2^{+/+}$ and $Nrf2^{-/-}$ mice ($P < 0.05$).

activation of immune-related transcription factors and the expression of proinflammatory cytokines and chemokines in peritoneal macrophages obtained from WT mice and $Nrf2^{-/-}$ mice in response to CSE or poly(I:C). The nuclear translocation of NF-κB and IRF-3 proteins increased in a dose-dependent manner in $Nrf2^{-/-}$ macrophages 6 h after exposure to CSE. Similar results were seen with $Nrf2^{-/-}$ macrophages after exposure to 5% CSE at the same time point (Fig. 1A), while there was no difference in nuclear translocation in WT macrophages after exposure to CSE (Fig. 1A). However, the nuclear translocation of Nrf2 increased in WT macrophages 6 h after exposure to CSE in a dose-dependent manner (Fig. 1A). As expected, Nrf2 was not detected in $Nrf2^{-/-}$ macrophages.

The nuclear translocation of the NF-κB and IRF-3 proteins increased in both WT and $Nrf2^{-/-}$ macrophages 6 h after exposure to poly(I:C). However, there was no difference in the levels of NF-κB between WT and $Nrf2^{-/-}$ macrophages (Fig. 1B) and only a slight increase in nuclear IRF-3 levels in $Nrf2^{-/-}$ macrophages after treatment with 30 μg/ml poly(I:C) (Fig. 1B). The level of nuclear translocation of Nrf2 slightly increased in WT macrophages in response to poly(I:C) stimulation (Fig. 1B).

The expression of TNF-α and MIP-2 mRNAs increased significantly in $Nrf2^{-/-}$ macrophages 24 h after exposure to 5% CSE (Fig. 1C), with significantly higher increases observed for $Nrf2^{-/-}$ macrophages than for WT macrophages (Fig. 1C). The IFN-β mRNA expression level was also significantly increased in $Nrf2^{-/-}$ macrophages after exposure to 2.5% and 5% CSE, compared with CSE-unexposed control and WT macrophages (Fig. 1C). The expression levels of TNF-α and MIP-2 mRNAs increased after 24 h of exposure to poly(I:C) in both WT and $Nrf2^{-/-}$ macrophages. The expression level was

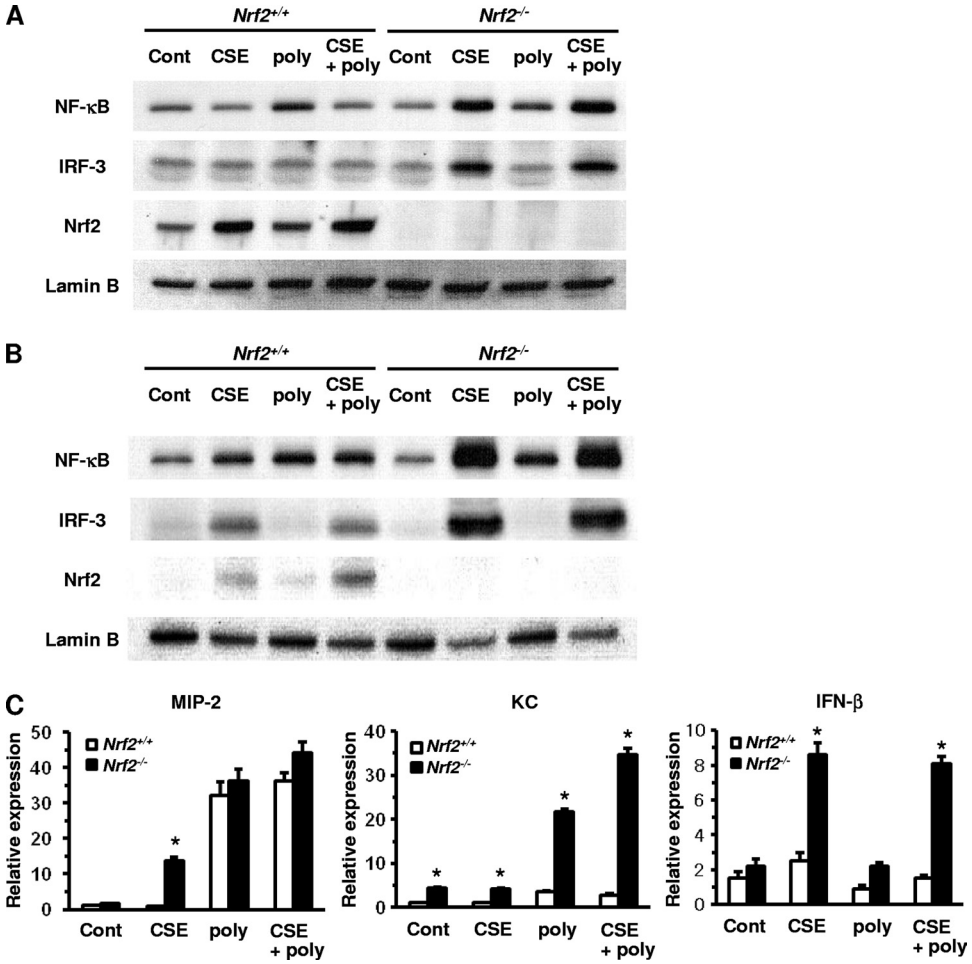

FIG. 2. Activation of transcription factors and induction of their targeted cytokine/chemokine genes in peritoneal macrophages after costimulation with cigarette smoke extract (CSE) and poly(I:C). (A and B) Nuclear translocation of the transcription factors NF-κB, IRF-3, and Nrf2 in peritoneal macrophages of $Nrf2^{+/+}$ and $Nrf2^{-/-}$ mice 6 h (A) and 24 h (B) after exposure to 5% CSE, 3 μg/ml poly(I:C) (poly), or both (CSE+poly). Lamin B was used as an internal control (Cont). (C) mRNA expressions of MIP-2, KC, and IFN-β in peritoneal macrophages of $Nrf2^{+/+}$ and $Nrf2^{-/-}$ mice after exposure to 5% CSE, 3 μg/ml poly(I:C) (poly), or both (CSE+poly). Each expression was normalized against GAPDH mRNA. Data are expressed as the means ± SEM ($n = 3$). *, significant difference between $Nrf2^{+/+}$ and $Nrf2^{-/-}$ mice ($P < 0.05$).

significantly higher in $Nrf2^{-/-}$ macrophages than in WT macrophages following exposure to 3 μg/ml poly(I:C) (Fig. 1D). The level of expression of IFN-β mRNA increased in $Nrf2^{-/-}$ macrophages but not in WT macrophages after 24 h of exposure to poly(I:C), with significant differences in expression observed after exposure to 3 and 30 μg/ml poly(I:C) (Fig. 1D). These results indicate that $Nrf2^{-/-}$ macrophages are more sensitive to CSE and poly(I:C) in terms of their induction of immune- and inflammatory-related genes.

Effects of Nrf2 on NF-κB-mediated inflammatory gene expression in CSE- and poly(I:C)-exposed macrophages. To assess the effect of Nrf2 on poly(I:C)-activated signaling pathways under conditions of oxidative stress, macrophages were cotreated with 5% CSE and 3 μg/ml poly(I:C). In WT macrophages, NF-κB was activated by poly(I:C), but not by CSE, 6 h after treatment (Fig. 2A). The poly(I:C)-stimulated activation of NF-κB was attenuated by cotreatment with CSE (Fig. 2A). However, NF-κB was activated by poly(I:C), CSE, or both 24 h after treatment in these cells (Fig. 2B). On the other hand, the activation of NF-κB was CSE dependent in $Nrf2^{-/-}$ macrophages both 6 h and 24 h after the treatment, with marked increases in the nuclear translocation of NF-κB and protein following exposure to CSE or after cotreatment with CSE and poly(I:C) (Fig. 2A and B). Although an obvious activation of IRF-3 was not observed 6 h after treatment with poly(I:C) or CSE, its nuclear translocation was enhanced 24 h after exposure to CS or cotreatment with CSE and poly(I:C) in WT macrophages (Fig. 2A and B). The activation of IRF-3 was greatly enhanced 6 h and 24 h following exposure to CSE or after cotreatment with CSE and poly(I:C) in $Nrf2^{-/-}$ macrophages (Fig. 2A and B). The activation of Nrf2 was also CSE dependent in WT macrophages; the nuclear translocation of Nrf2 was enhanced after exposure to CSE or after cotreatment with CSE and poly(I:C) both 6 h and 24 h after treatment (Fig. 2A and B). Nrf2 was not detected in $Nrf2^{-/-}$ macrophages at any time point (Fig. 2A and B).

We then assessed the expressions of NF-κB and IRF-3 target genes 24 h after cotreatment with CSE and poly(I:C).

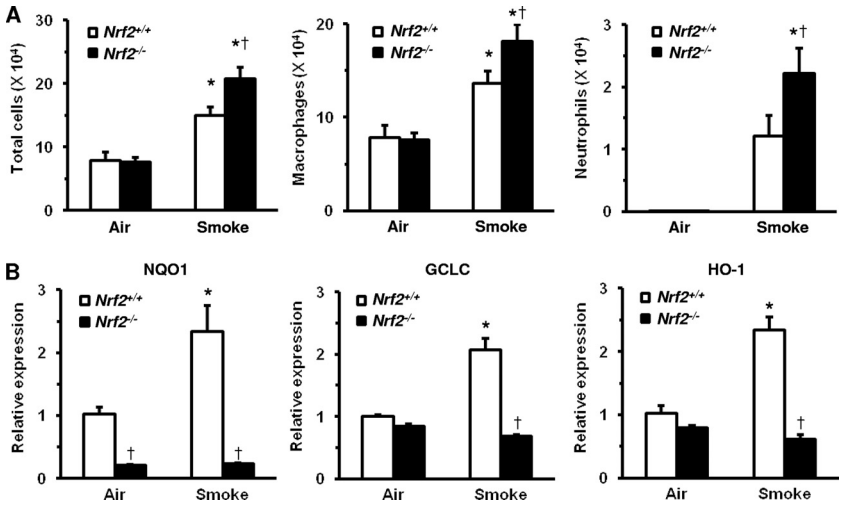

FIG. 3. Effects of cigarette smoke exposure on pulmonary inflammation and Nrf2-targeted gene expression. (A) Numbers of total cells (left), macrophages (center), and neutrophils (right) in bronchoalveolar lavage fluids of wild-type ($Nrf2^{+/+}$) mice and Nrf2-deficient ($Nrf2^{-/-}$) mice after exposure to cigarette smoke or air. Data are expressed as the means ± SEM (n = 5 to 13). ⋆, significant difference compared with the corresponding air-exposed control ($P < 0.05$). †, significant difference between $Nrf2^{+/+}$ and $Nrf2^{-/-}$ mice ($P < 0.05$). (B) mRNA expressions of NQO1, GCLC, GCLM, and HO-1 in the lungs of $Nrf2^{+/+}$ and $Nrf2^{-/-}$ mice after exposure to cigarette smoke or air. Each expression was normalized against GAPDH mRNA. Data are expressed as the means ± SEM (n = 4). ⋆, significant difference compared with the corresponding air-exposed control ($P < 0.05$). †, significant difference between $Nrf2^{+/+}$ and $Nrf2^{-/-}$ mice ($P < 0.05$).

Although the levels of expression of MIP-2 mRNA markedly increased in both WT and $Nrf2^{-/-}$ macrophages after treatment with poly(I:C), the expression level was not different between genotypes regardless of CSE treatment (Fig. 2C). However, marked increases in the levels of expression of KC mRNA were seen specifically for $Nrf2^{-/-}$ macrophages after treatment with poly(I:C) or cotreatment with CSE and poly(I:C) (Fig. 2C). The expression level was higher after cotreatment with CSE and poly(I:C) than after treatment with poly(I:C) alone (Fig. 2C). The expression of IFN-β paralleled the nuclear translocation of IRF-3 in $Nrf2^{-/-}$ macrophages; the expression level was markedly increased after exposure to CSE or after cotreatment with CSE and poly(I:C) (Fig. 2C). The level of expression of IFN-β did not increase after the cotreatment for WT macrophages (Fig. 2C). These results indicate that oxidative conditions enhance the poly(I:C)-mediated activation of NF-κB and IRF-3 and the induction of their targeted genes in $Nrf2^{-/-}$ macrophages.

Protective effects of Nrf2 on CS-induced pulmonary inflammation. To clarify the effects of Nrf2 on CS-induced pulmonary inflammation, WT mice and $Nrf2^{-/-}$ mice were exposed to CS. Although the numbers of total cells, macrophages, and neutrophils were increased in the BAL fluids of WT and $Nrf2^{-/-}$ mice after exposure to CS for 4 consecutive days, cell numbers were significantly higher in $Nrf2^{-/-}$ mice than in WT mice (Fig. 3A).

To reveal whether the protective effects of Nrf2 are mediated through the transactivation of its targeted cellular defense genes, the expressions of NQO1, GCLC, GCLM, and HO-1 mRNAs in the lungs of WT and $Nrf2^{-/-}$ mice after exposure to CS were evaluated. A significant increase in their mRNA expression levels was found for the lungs of WT mice in response to CS stimuli (Fig. 3B). The expression levels of NQO1, GCLC, GCLM, and HO-1 were also significantly lower in $Nrf2^{-/-}$ mice than in WT mice after exposure to CS (Fig. 3B). These results indicate that Nrf2 helps to protect against the development of CS-induced pulmonary inflammation by mediating the induction of antioxidant genes.

Protective effects of Nrf2 on FluV infection exacerbations induced by CS. Since the activation of NF-κB and the expression of its targeted inflammatory genes were enhanced after cotreatment with CSE and poly(I:C) in $Nrf2^{-/-}$ macrophages, the severity of FluV infection was examined with WT and $Nrf2^{-/-}$ mice with or without exposure to CS. There was no significant difference in mortality rates between WT and $Nrf2^{-/-}$ mice after FluV infection alone (57% and 74%, respectively) (Fig. 4A). The mortality rate for the CS-plus-FluV group was increased significantly over that for the FluV group of WT and $Nrf2^{-/-}$ mice. In the CS-plus-FluV groups, the mortality rate was significantly higher for $Nrf2^{-/-}$ mice than for WT mice; all of the $Nrf2^{-/-}$ mice died by day 10, whereas there were still WT mice alive at day 14 (Fig. 4A).

The severity of FluV infection was also evaluated by monitoring changes in the body weights of mice of both genotypes. Body weight loss was observed for WT and $Nrf2^{-/-}$ mice 7 days after FluV infection (Fig. 4B). In $Nrf2^{-/-}$ mice, FluV infection-caused body weight loss was significantly greater in the CS-plus-FluV group than in the FluV group, and this was significantly greater than that in CS- and FluV-treated WT mice (Fig. 4B). These results indicate that FluV infection exacerbations induced by CS exposure are much more severe in $Nrf2^{-/-}$ mice.

To clarify whether Nrf2 directly affects the replication and clearance of FluV, the viral load was evaluated 1, 3, and 7 days after FluV infection with or without exposure to CS in the lungs of WT and $Nrf2^{-/-}$ mice. There was no difference in the viral loads between WT mice and $Nrf2^{-/-}$ mice at any time point, and there was no effect of CS exposure.

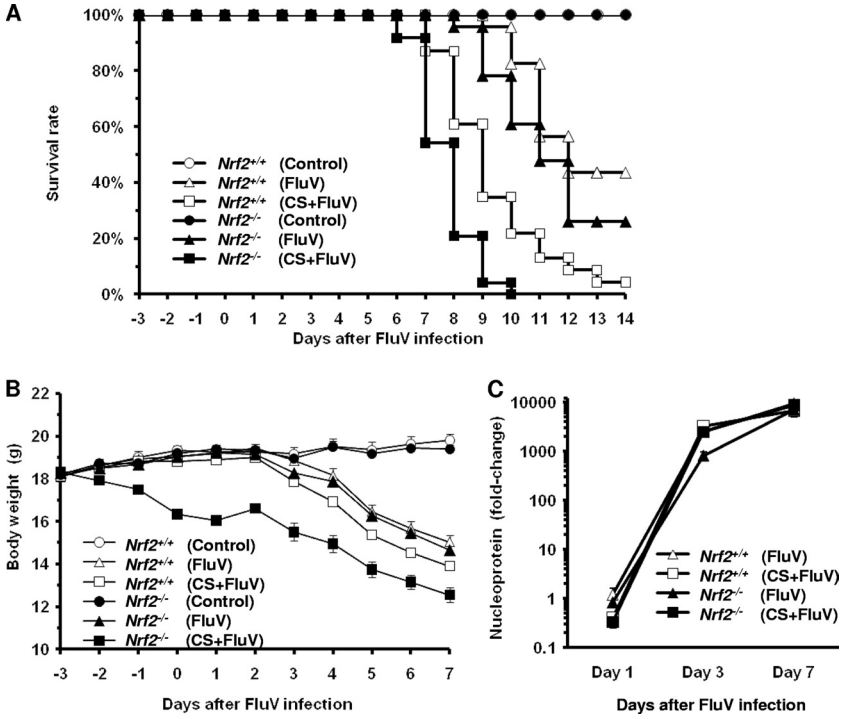

FIG. 4. Effect of cigarette smoke exposure on the severity of influenza virus infection. (A) Survival of wild-type ($Nrf2^{+/+}$) (open symbols) mice and Nrf2-deficient ($Nrf2^{-/-}$) (closed symbols) mice after intranasal inoculation of influenza virus (FluV) with (squares) or without (triangles) exposure to cigarette smoke (CS). Control mice were inoculated with physiological saline (circles) ($n = 18$ to 24). There was a significant difference between $Nrf2^{+/+}$ and $Nrf2^{-/-}$ mice in the CS-plus-FluV group ($P < 0.05$). (B) Changes in body weight in wild-type ($Nrf2^{+/+}$) (open symbols) mice and Nrf2-deficient ($Nrf2^{-/-}$) (closed symbols) mice after intranasal inoculation of influenza virus (FluV) with (squares) or without (triangles) exposure to CS ($n = 10$ in each group). There was a significant difference between $Nrf2^{+/+}$ and $Nrf2^{-/-}$ mice in the CS-plus-FluV group ($P < 0.05$). (C) Viral loads in the lung tissues of wild-type ($Nrf2^{+/+}$) (open symbols) mice and Nrf2-deficient ($Nrf2^{-/-}$) (closed symbols) mice after intranasal inoculation of influenza virus (FluV) with (squares) or without (triangles) exposure to CS ($n = 4$ to 8).

Activation of Nrf2 in alveolar macrophages. To clarify whether Nrf2 is activated in the lung tissue after FluV infection of CS-exposed mice, immunohistochemical analysis was performed 7 days post-FluV infection for the CS-plus-FluV groups. Strong Nrf2 staining was observed for alveolar macrophages (Fig. 5B) but not for the bronchial epithelial cells (Fig. 5A) of WT mice. In contrast, there was no Nrf2 staining observed for $Nrf2^{-/-}$ lung tissue (Fig. 5A and B), indicating that the activation of Nrf2 occurs mainly in alveolar macrophages after costimulation with FluV and CS.

Increase in oxidative stress and inflammatory gene expression post-FluV infection in CS-exposed $Nrf2^{-/-}$ mice. To clarify whether oxidative stress is enhanced in the lungs of $Nrf2^{-/-}$ mice, the production of 8-OHdG, a cellular oxidative stress marker, was evaluated immunohistochemically 7 days post-FluV infection. Positive staining for 8-OHdG was observed for WT and $Nrf2^{-/-}$ mice in the FluV and CS-plus-FluV groups, particularly in alveolar macrophages (Fig. 6A). The strongest staining was observed for the alveolar macrophages of $Nrf2^{-/-}$ mice in the CS-plus-FluV group (Fig. 6A). There was no staining observed for the lungs of either control group (Fig. 6A).

Since the expression of inflammatory genes, such as TNF-α and KC, was enhanced in cultured $Nrf2^{-/-}$ macrophages by stimulation with CSE and poly(I:C), we then evaluated their mRNA expression levels in BAL fluid cells and protein levels in BAL fluids of WT mice and $Nrf2^{-/-}$ mice 7 days post-FluV infection. The expression levels of both TNF-α and KC mRNAs were significantly increased for both genotypes in the FluV and CS-plus-FluV groups (Fig. 6B). In contrast to WT mice, $Nrf2^{-/-}$ mice exhibited a significant increase in the expression levels of TNF-α and KC mRNAs in the CS-plus-FluV group compared to the FluV group (Fig. 6B). In the CS-plus-FluV group, the level of KC mRNA was significantly higher in $Nrf2^{-/-}$ mice than in WT mice (Fig. 6B). The concentrations of both TNF-α and KC were also significantly increased for both genotypes in the FluV and CS-plus-FluV groups (Fig. 6C). The concentration of KC was significantly higher in the BAL fluids of $Nrf2^{-/-}$ mice than in those of WT mice in the FluV and the CS-plus-FluV groups (Fig. 6C).

We then assessed the lung histopathologies of both genotypes after FluV infection with or without exposure to CS. Inflammatory cells, both polymorphonuclear leukocytes and mononuclear cells, were infiltrated throughout the airspaces 7 days post-FluV infection in both WT mice and $Nrf2^{-/-}$ mice. The inflammatory cell infiltration was most prominently observed for the peribronchial and perivascular regions with subepithelial edema (Fig. 7A). Mucus was layered with degenerative epithelial cells in the bronchial lumen. These pathological changes were more severe for the CS-plus-FluV groups than for the FluV groups of both genotypes, with more severe phenotypes for the CS-plus-FluV group of $Nrf2^{-/-}$ mice than for WT mice (Fig. 7A). We next determined the levels of nuclear

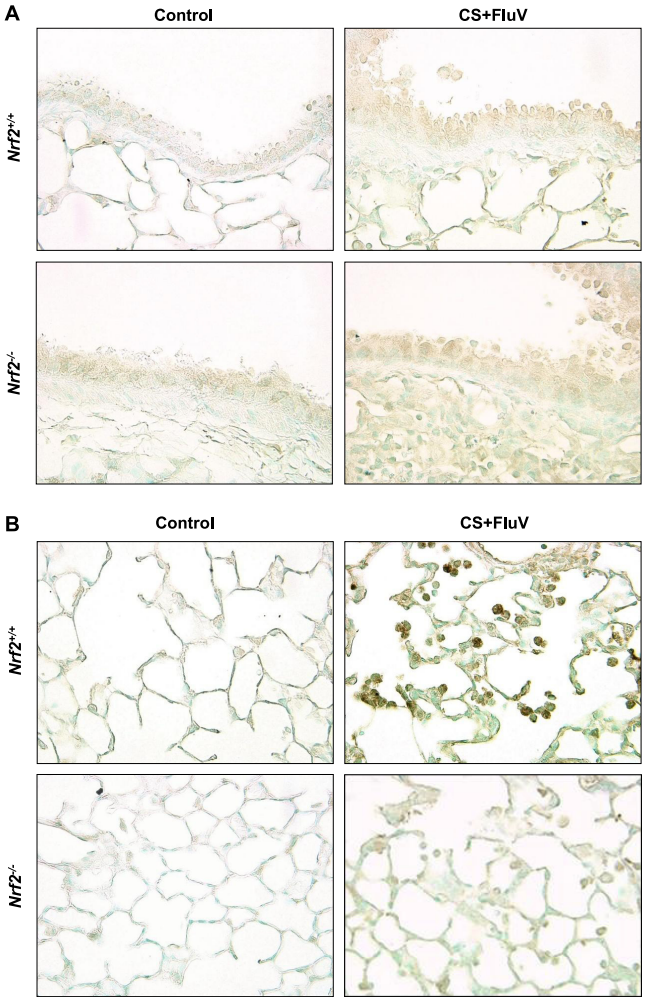

FIG. 5. Immunohistochemical staining of Nrf2 in the bronchial (A) and alveolar (B) regions. The lungs were obtained from wild-type ($Nrf2^{+/+}$) mice and Nrf2-deficient ($Nrf2^{-/-}$) mice 7 days after the intranasal inoculation of influenza virus with exposure to cigarette smoke. Positive staining for Nrf2 was visible in the alveolar regions in alveolar macrophages but not in the bronchial epithelium of $Nrf2^{+/+}$ mice. No positive cells were observed in any region for the $Nrf2^{-/-}$ mice. Sections were counterstained with methyl green. Original magnification, ×200.

NF-κB translocation in the lungs of both genotypes using Western blot analysis. The level of nuclear translocation of NF-κB was elevated in the lungs of both genotypes in the FluV and CS-plus-FluV groups, with increased translocation observed for the CS-plus-FluV group of $Nrf2^{-/-}$ mice compared to WT mice (Fig. 7B). We then assessed the concentrations of the NF-κB target proteins TNF-α and KC in the lungs of WT mice and $Nrf2^{-/-}$ mice at 7 days post-FluV infection. The concentrations of TNF-α and KC were also increased in the lungs of both genotypes in the FluV and CS-plus-FluV groups (Fig. 7C). In $Nrf2^{-/-}$ mice, the concentrations of TNF-α and KC were significantly higher in the CS-plus-FluV group than in the FluV group, which were again higher than those in the corresponding groups of the WT mice (Fig. 7C). These results indicate that NF-κB-mediated inflammatory gene expression and pulmonary inflammation, dominantly occurring in the peribronchial region, are enhanced in the lungs of CS-exposed $Nrf2^{-/-}$ mice after FluV infection.

Protective effects of Nrf2 on FluV-induced lung permeability damage after CS exposure. FluV-induced lung permeability damage causes increased severity and mortality. We therefore assessed the protein concentrations in BAL fluids and the lung wet-to-dry weight ratio, both indicators of lung permeability damage, of WT mice and $Nrf2^{-/-}$ mice at 7 days post-FluV infection. The protein levels in BAL fluids were markedly increased in WT and $Nrf2^{-/-}$ mice of the FluV and CS-plus-FluV groups compared with the levels in the corresponding control group (Fig. 8A). For each genotype, the protein concentration was significantly higher in the CS-plus-FluV group than in the FluV group, with the level in $Nrf2^{-/-}$ mice being significantly higher than that in the WT mice (Fig. 8A).

Similarly, the lung wet-to-dry weight ratio was significantly increased in the CS- and FluV-treated WT and $Nrf2^{-/-}$ mice compared with that of the FluV groups (Fig. 8B), and this was significantly higher in $Nrf2^{-/-}$ mice than in WT mice in the CS-plus-FluV group (Fig. 8B). These results indicate that lung permeability damage is enhanced in the lungs of CS-exposed $Nrf2^{-/-}$ mice after FluV infection.

Protective effects of Nrf2 on FluV-induced mucus hyperproduction after CS exposure. Mucus hyperproduction and hypersecretion are some of the characteristic pathological features of an acute exacerbation of COPD. We therefore assessed the degree of mucus production in the airways of WT and $Nrf2^{-/-}$ mice 7 days post-FluV infection. Mucus-producing PAS-positive cells were scarcely seen in the airway epithelium of each control group. Although the numbers of PAS-positive cells increased for both genotypes of mice after FluV infection, the number of PAS-positive cells was increased in the CS-plus-FluV group compared with the numbers for the corresponding FluV group (Fig. 9A). Numbers of PAS-positive cells in the CS-plus-FluV group of $Nrf2^{-/-}$ mice were increased over those in WT mice (Fig. 9A).

The degree of mucus secretion was also assessed by the measurement of MUC5AC in BAL fluids. The level of MUC5AC was significantly elevated in WT and $Nrf2^{-/-}$ mice after FluV infection (Fig. 9B). In the CS-plus-FluV group, the level of MUC5AC was significantly higher in $Nrf2^{-/-}$ mice than in WT mice (Fig. 9B). These results indicate that mucus production and secretion are enhanced in the epithelium of CS-exposed $Nrf2^{-/-}$ mice after FluV infection.

DISCUSSION

In the present study, we demonstrated that mice lacking Nrf2 are highly susceptible to FluV infection under conditions of CS exposure. Nrf2 is a pivotal factor involved in cellular protection against oxidative stimuli, inducing several antioxidant genes. Correspondingly, the production of 8-OHdG, an oxidative stress marker, was enhanced in the lungs of $Nrf2^{-/-}$ mice after exposure to FluV and CS. Moreover, the induction of antioxidant and phase II enzyme genes, found in the macrophages of WT mice in response to CS exposure, was not observed for $Nrf2^{-/-}$ mice. These results suggest that the impairment of antioxidant defense contributes to the enhancement of FluV-induced pulmonary inflammation and injury under conditions of CS exposure in $Nrf2^{-/-}$ mice.

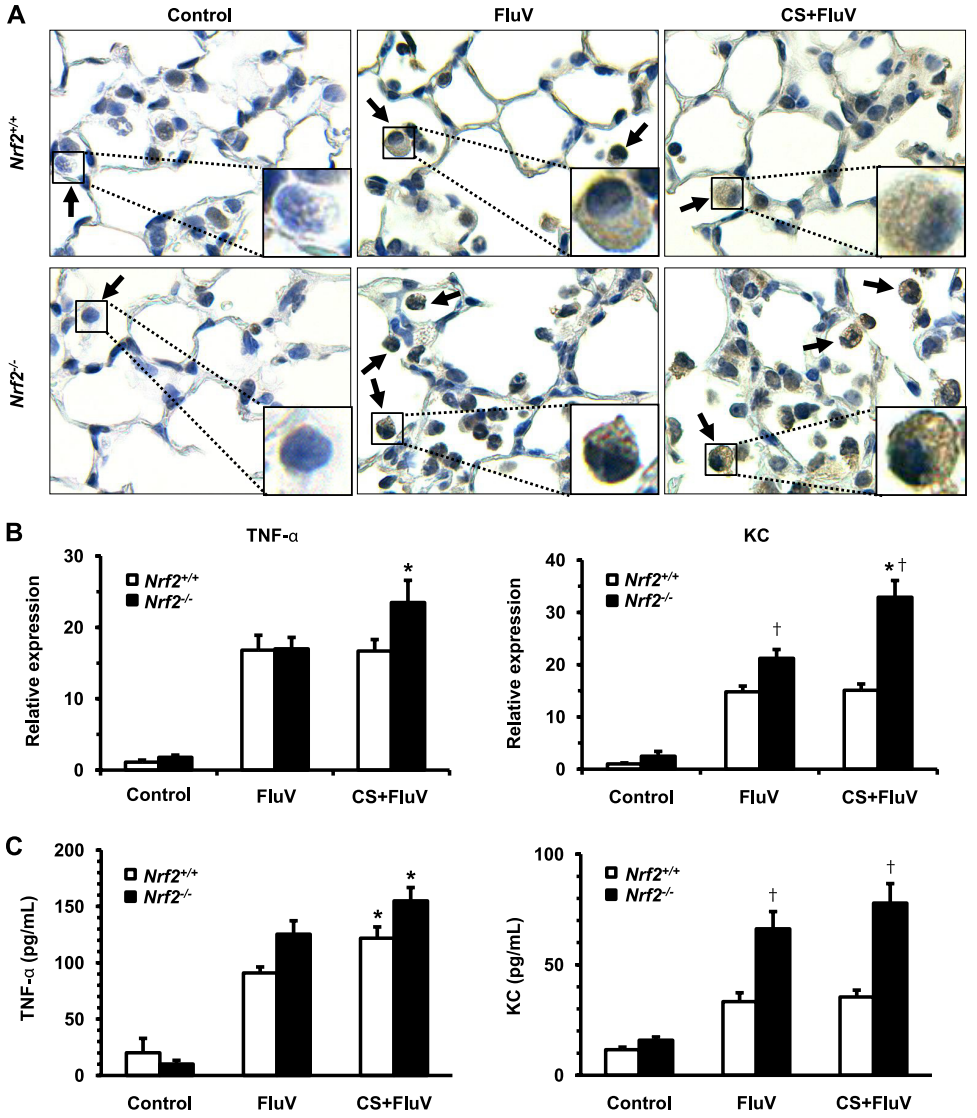

FIG. 6. Increase in oxidative stress and inflammatory gene expression in alveolar cells. (A) Immunohistochemical staining of 8-OHdG, an oxidative stress marker, in the lungs of wild-type ($Nrf2^{+/+}$) mice and Nrf2-deficient ($Nrf2^{-/-}$) mice 7 days after intranasal inoculation of influenza virus (FluV) with or without exposure to cigarette smoke (CS). Control mice were inoculated with physiological saline. 8-OHdG was most prominently detected in alveolar macrophages (arrows and insets). Sections were counterstained with hematoxylin. Original magnification, ×200. (B) mRNA expressions of TNF-α and KC in the bronchoalveolar lavage fluid cells of $Nrf2^{+/+}$ and $Nrf2^{-/-}$ mice 7 days after intranasal inoculation of FluV with or without exposure to CS. Control mice were inoculated with physiological saline. mRNA expression was normalized against GAPDH mRNA. Data are expressed as the means ± SEM ($n = 4$ to 6). (C) Concentrations of TNF-α and KC in the bronchoalveolar lavage fluids of $Nrf2^{+/+}$ and $Nrf2^{-/-}$ mice 7 days after intranasal inoculation of FluV with or without exposure to CS. Control mice were inoculated with physiological saline. Data are expressed as the means ± SEM ($n = 8$ to 14). *, significant difference between FluV and CS-plus-FluV groups ($P < 0.05$). †, significant difference between $Nrf2^{+/+}$ and $Nrf2^{-/-}$ mice ($P < 0.05$).

We demonstrated that the activation of NF-κB and the induction of its targeted genes, such as TNF-α and KC, were enhanced in $Nrf2^{-/-}$ mice after exposure to FluV and CS. NF-κB is a transcription factor that plays a key role in the expression of various inflammatory genes, such as proinflammatory cytokines, adhesion molecules, chemokines, and respiratory mucins, in response to CS stimuli (1). It was also demonstrated previously that viral infection upregulates a plethora of proinflammatory molecules, such as CXC and CC chemokines, in an NF-κB-dependent manner (30, 42). Taken together, the induction of NF-κB-mediated inflammatory gene expression should be enhanced by CS exposure and viral infection. Thus, the activation of NF-κB may contribute largely to viral infection-triggered exacerbations of oxidant-induced lung diseases such as COPD.

Although NF-κB is expressed in a variety of cells, it was reported previously that the activation of NF-κB was observed for macrophages but not for neutrophils during COPD exacerbations (7). These results suggest that macrophages play an important role in NF-κB-mediated pulmonary inflammation. Viral infection, including FluV, activates NF-κB through several mechanisms. Viral dsRNA activates NF-κB by binding to

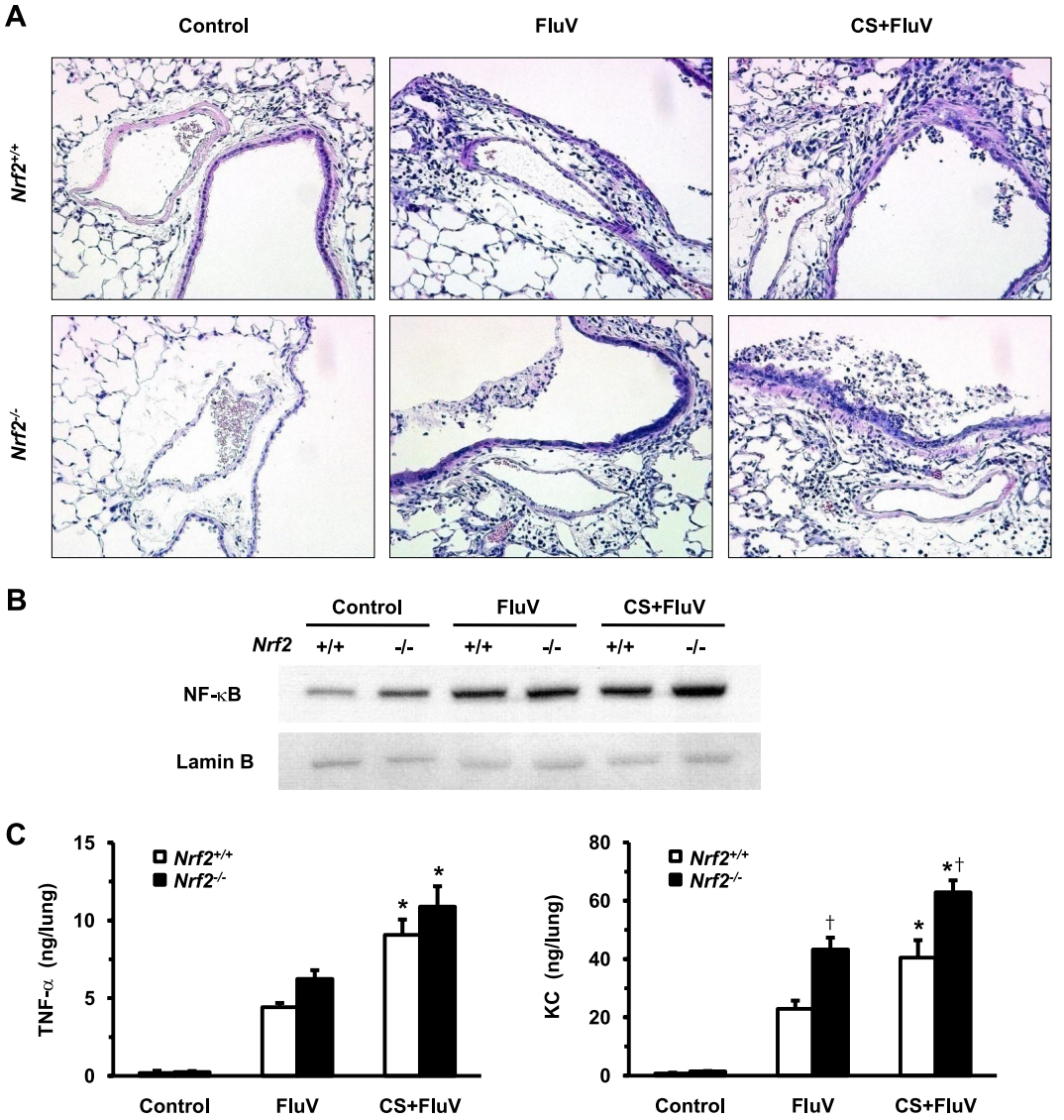

FIG. 7. Increase in pulmonary inflammation and NF-κB-mediated inflammatory gene expression in lungs after influenza virus infection. (A) Representative microphotographs of lung tissues of wild-type ($Nrf2^{+/+}$) mice and Nrf2-deficient ($Nrf2^{-/-}$) mice 7 days after intranasal inoculation of influenza virus (FluV) with or without exposure to cigarette smoke (CS). Control mice were inoculated with physiological saline. Inflammatory cell infiltration was observed throughout the lung but most prominently in peribronchial and perivascular regions with subepithelial edema in the CS-plus-FluV groups. Original magnification, ×100. (B) Nuclear translocation of the transcription factor NF-κB in lungs of wild-type ($Nrf2^{+/+}$) mice and Nrf2-deficient ($Nrf2^{-/-}$) mice 3 days after intranasal inoculation of influenza virus (FluV) with or without exposure to CS. Control mice were inoculated with physiological saline. Lamin B was used as an internal control. (C) Concentrations of TNF-α and KC in the lungs of $Nrf2^{+/+}$ and $Nrf2^{-/-}$ mice 7 days after intranasal inoculation of FluV with or without exposure to CS. Control mice were inoculated with physiological saline. Data are expressed as the means ± SEM (n = 5 to 6). *, significant difference between FluV and CS-plus-FluV groups ($P < 0.05$). †, significant difference between $Nrf2^{+/+}$ and $Nrf2^{-/-}$ mice ($P < 0.05$).

TLR3, a pattern recognition receptor (PRR) located on endosomal membranes, or through binding to retinoic acid-inducible gene I (RIG-I)-like receptors (RLRs), such as RIG-I and melanoma differentiation-associated gene 5 (MDA-5) (19, 20). Since macrophages dominantly express PRRs, FluV may activate NF-κB via exploiting TLR3 signaling pathways. Consistently, in the present study, the treatment of macrophages with poly(I:C), a synthetic analog of viral dsRNA that binds to TLR3, could activate NF-κB in both types of mice. It is of interest that the activation of NF-κB and IRF-3 and the induction of their targeted genes, such as TNF-α and IFN-β, were greater in $Nrf2^{-/-}$ macrophages than in WT macrophages after treatment with poly(I:C) alone. It was demonstrated previously that TLR signaling generates ROS via activating the NADPH oxidase complex, a major source of intracellular ROS generation (4). A recent study also demonstrated that NADPH oxidase-dependent ROS generation was greater in $Nrf2^{-/-}$ macrophages than in WT macrophages (22). It is therefore likely that higher levels of ROS amplify the activation of NF-κB in poly(I:C)-treated $Nrf2^{-/-}$ macrophages, since NF-κB is a redox-sensitive transcription factor. It was also demonstrated previously that IRF-3 is activated by

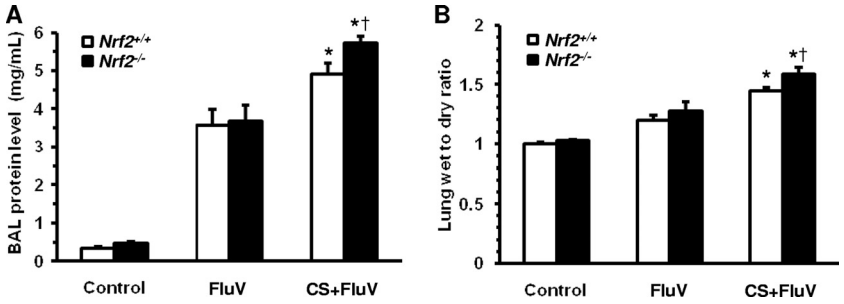

FIG. 8. Assessment of lung permeability damage after influenza virus infection. (A) Total protein concentration in bronchoalveolar lavage fluids obtained from wild-type ($Nrf2^{+/+}$) mice and Nrf2-deficient ($Nrf2^{-/-}$) mice 7 days after intranasal inoculation of influenza virus (FluV) with or without exposure to cigarette smoke (CS). Control mice were inoculated with physiological saline. Data are expressed as the means ± SEM (n = 6 to 8). (B) Lung wet-to-dry weight ratio 7 days after intranasal inoculation of FluV with or without exposure to CS. Control mice were inoculated with physiological saline. Data are expressed as the means ± SEM (n = 5). *, significant difference between FluV and CS-plus-FluV groups ($P < 0.05$). †, significant difference between $Nrf2^{+/+}$ and $Nrf2^{-/-}$ mice ($P < 0.05$).

ROS (8). In the present study, Nrf2 did not affect the expression level of TLR3 in macrophages (data not shown).

Similar to poly(I:C) stimulation, the activation of NF-κB and IRF-3 and the induction of their targeted genes were increased in $Nrf2^{-/-}$ macrophages after CSE stimulation. Moreover, the increase in NF-κB activation was enhanced in $Nrf2^{-/-}$ macrophages after cotreatment with poly(I:C) and CSE compared with that after treatment with poly(I:C) alone, while the activation of NF-κB was diminished in WT macrophages after cotreatment with poly(I:C) and CSE compared with that of

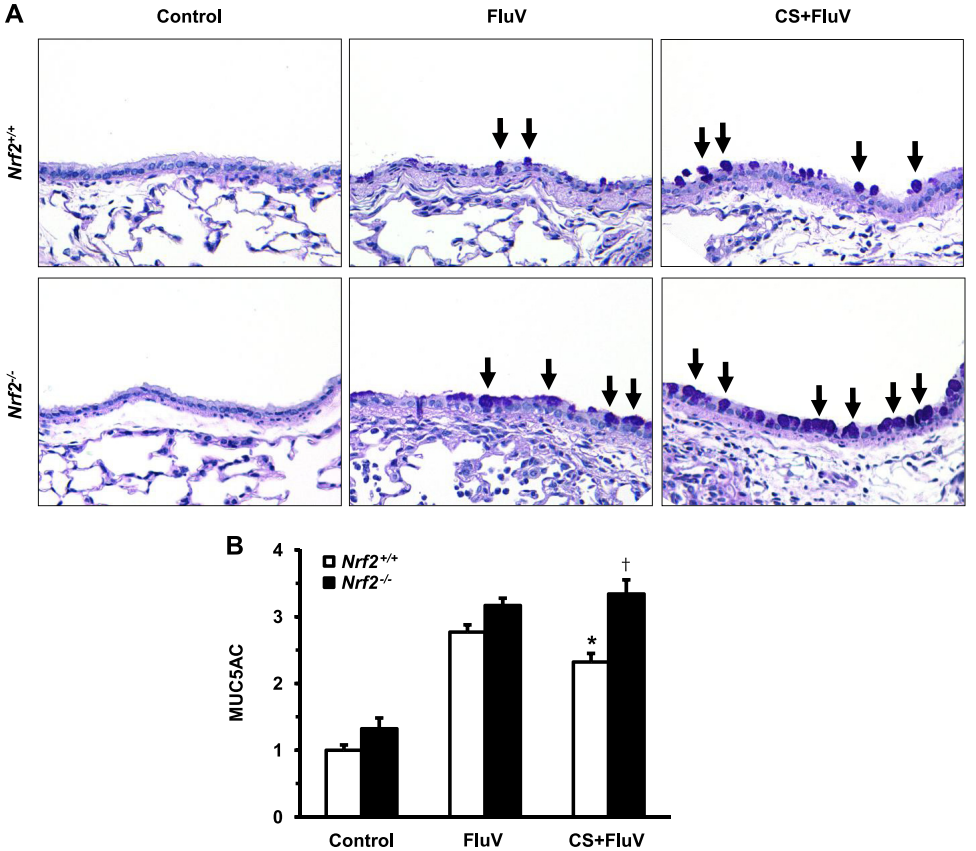

FIG. 9. Assessment of mucus production after influenza virus infection. (A) Representative microphotographs of lung tissues of wild-type ($Nrf2^{+/+}$) mice and Nrf2-deficient ($Nrf2^{-/-}$) mice 7 days after intranasal inoculation of influenza virus (FluV) with or without exposure to cigarette smoke (CS). Control mice were inoculated with physiological saline. PAS-positive cells (arrows) were visible in the epithelium after viral infection. Original magnification, ×200. (B) MUC5AC levels in bronchoalveolar lavage fluids obtained from $Nrf2^{+/+}$ and $Nrf2^{-/-}$ mice 7 days after intranasal inoculation of FluV with or without exposure to CS. Control mice were inoculated with physiological saline. The graph shows the fold increase of the relative MUC5AC level from the value for $Nrf2^{+/+}$ control mice. Data are expressed as the means ± SEM (n = 5). *, significant difference between FluV and CS-plus-FluV groups ($P < 0.05$). †, significant difference between $Nrf2^{+/+}$ and $Nrf2^{-/-}$ mice ($P < 0.05$).

poly(I:C) treatment alone. CS is a complex mixture of various noxious gases and condensed particles that contain various ROS and inflammatory mediators. CS therefore induces oxidative stress followed by the activation of NF-κB by activating the stress-sensitive IκB kinase (2). In WT macrophages, the level of nuclear translocation of Nrf2 was found to be increased after treatment with CSE, suggesting that the activation of Nrf2 in response to oxidative stimuli efficaciously inhibits the virus-induced activation of NF-κB in normal cells. On the other hand, oxidative stimuli may strongly amplify the virus-induced activation of NF-κB and the induction of its targeted inflammatory genes if cells lack Nrf2.

Immunohistochemistry revealed that strong Nrf2 staining was observed for alveolar macrophages but not for bronchial epithelial cells after FluV infection of CS-exposed WT mice. These findings suggest that the Nrf2-mediated defense system acts mainly on macrophages in the lung tissue. This finding is consistent with our previously reported findings with CS-induced or elastase-induced emphysema models in which Nrf2-targeted antioxidant and antiprotease genes were strongly induced in alveolar macrophages (16, 17). As stated above, both dsRNA- and CS-induced NF-κB activation and its mediated production of inflammatory mediators occur in macrophages. It was previously demonstrated that both FluV infection and CS exposure can generate ROS in phagocytic cells, including macrophages (27). It is therefore likely that the macrophage-specific activation of Nrf2 efficaciously inhibits the NF-κB-mediated inflammatory cascade by reducing cellular ROS levels. In the present study, we found that the levels of markers of oxidative stress and the nuclear translocation of NF-κB were much enhanced in the macrophages of CS-exposed *Nrf2*$^{-/-}$ mice after FluV infection.

Our data demonstrated that the mortality rate of *Nrf2*$^{-/-}$ mice was significantly higher than that of WT mice in the CS-plus-FluV group. In this group, *Nrf2*$^{-/-}$ mice exhibited severe inflammation throughout the lungs. Seasonal influenza A viruses, including H1N1, cause inflammation primarily in the larger airways. However, inflammation and injury may spread to lower airways during severe and fatal influenza virus infection (15). It is therefore possible that smokers who have low levels of Nrf2 activity are a high-risk group for severe influenza virus infection. Other researchers demonstrated previously that the level of Nrf2 expression was decreased in the macrophages of older current smokers and patients with COPD (23, 32). Viral infection is the leading cause of COPD exacerbations (23, 32). In the present study, CS-exposed *Nrf2*$^{-/-}$ mice showed severe pulmonary inflammation, lung permeability damage, and mucus hypersecretion after FluV infection. These phenotypes are characteristic pathological findings of an acute exacerbation of COPD. Taken together, Nrf2 is suggested to be a pivotal host factor in protection against virus-induced COPD exacerbations.

It was demonstrated previously that *Nrf2*$^{-/-}$ mice were also susceptible to experimental sepsis induced by lipopolysaccharide, a TLR4 ligand (35), and to pulmonary inflammation induced by respiratory syncytial virus (RSV) (11), associated with the enhanced activation of NF-κB. Although an enhanced viral load in *Nrf2*$^{-/-}$ mice contributed to the deterioration of airway inflammation in RSV infection (11), Nrf2 may not directly affect the replication and clearance of FluV, since the viral load of WT mice was not different from that of *Nrf2*$^{-/-}$ mice after FluV infection in the present model. Moreover, the severities of pulmonary inflammation after FluV infection alone were not different between WT mice and *Nrf2*$^{-/-}$ mice. These differences among viruses may be due to the types of virus or to the potency of ROS production.

In *Nrf2*$^{-/-}$ mice, the exacerbation of pulmonary inflammation and permeability damage was accompanied by increased levels of KC in BAL fluid cells or lung homogenates. KC, also called as CXCL1, is a mouse ortholog of human GRO-α, a potent neutrophil chemoattractant belonging to the CXC chemokine family (25). There is accumulating evidence that CXC chemokines play a role in pulmonary inflammation and lung damage during COPD exacerbations (13, 37). It was also reported previously that the lack of Nrf2 caused prolonged inflammatory cell infiltration into the lung with a prolonged expression of CXCL2 after hyperoxia (29). In this regard, Nrf2 is considered a critical factor for the resolution of pulmonary inflammation following oxidative stress by regulating CXC chemokine expression.

In the present study, mucus production and secretion were enhanced in CS-exposed *Nrf2*$^{-/-}$ mice after FluV infection. Mucus hypersecretion is a typical pathological finding in the airways of those with COPD exacerbations (36). In bronchial epithelial cells, the expression of MUC5AC, the major mucin protein, was regulated by TNF-α (31) and neutrophil elastase (14). CXC chemokines might also affect the expression of MUC5AC by recruiting and activating neutrophils. An excessive induction of TNF-α and KC may contribute, at least in part, to mucus hypersecretion in *Nrf2*$^{-/-}$ mice.

In conclusion, mice lacking Nrf2 were highly susceptible to FluV infection after CS exposure. CS-exposed *Nrf2*$^{-/-}$ mice showed severe pulmonary inflammation, lung permeability damage, and mucus hypersecretion after FluV infection, phenotypes which are similar to the pathological findings observed for the lungs during COPD exacerbations. Nrf2-mediated antioxidant pathways may play a pivotal role in protection against the oxidant-induced exacerbation of FluV infection by the upregulation of antioxidants, the inactivation of the redox-sensitive transcription factor NF-κB, and the dysregulation of NF-κB-mediated inflammatory mediators. Thus, Nrf2 might be a potential novel therapeutic target for the prevention of virus-induced exacerbations of inflammatory lung diseases such as COPD.

ACKNOWLEDGMENT

This work was supported by a grant-in-aid for scientific research (C) from the Japan Society for the Promotion of Science.

REFERENCES

1. **Ahn, K. S., and B. B. Aggarwal.** 2005. Transcription factor NF-kappaB: a sensor for smoke and stress signals. Ann. N. Y. Acad. Sci. **1056:**218–233.
2. **Anto, R. J., A. Mukhopadhyay, S. Shishodia, C. G. Gairola, and B. B. Aggarwal.** 2002. Cigarette smoke condensate activates nuclear transcription factor-kappaB through phosphorylation and degradation of IkappaB(alpha): correlation with induction of cyclooxygenase-2. Carcinogenesis **23:**1511–1518.
3. **Au, D. H., et al.** 2009. The effects of smoking cessation on the risk of chronic obstructive pulmonary disease exacerbations. J. Gen. Intern. Med. **24:**457–463.
4. **Bae, Y. S., et al.** 2009. Macrophages generate reactive oxygen species in response to minimally oxidized low-density lipoprotein: Toll-like receptor 4- and spleen tyrosine kinase-dependent activation of NADPH oxidase 2. Circ. Res. **104:**210–218.

5. **Bar, I., et al.** 2008. Knockout mice reveal a role for P2Y6 receptor in macrophages, endothelial cells, and vascular smooth muscle cells. Mol. Pharmacol. **74:**777–784.
6. **Bautista, E., et al.** 2010. Clinical aspects of pandemic 2009 influenza A (H1N1) virus infection. N. Engl. J. Med. **362:**1708–1719.
7. **Caramori, G., et al.** 2003. Nuclear localisation of p65 in sputum macrophages but not in sputum neutrophils during COPD exacerbations. Thorax **58:**348–351.
8. **Chiang, E., et al.** 2006. Apoptosis-regulating signal kinase 1 is required for reactive oxygen species-mediated activation of IFN regulatory factor 3 by lipopolysaccharide. J. Immunol. **176:**5720–5724.
9. **Cho, H. Y., S. P. Reddy, M. Yamamoto, and S. R. Kleeberger.** 2004. The transcription factor NRF2 protects against pulmonary fibrosis. FASEB J. **18:**1258–1260.
10. **Cho, H. Y., and S. R. Kleeberger.** 2007. Genetic mechanisms of susceptibility to oxidative lung injury in mice. Free Radic. Biol. Med. **42:**433–445.
11. **Cho, H. Y., et al.** 2009. Antiviral activity of Nrf2 in a murine model of respiratory syncytial virus disease. Am. J. Respir. Crit. Care Med. **179:**138–150.
12. **De Serres, G., et al.** 2009. Importance of viral and bacterial infections in chronic obstructive pulmonary disease exacerbations. J. Clin. Virol. **46:**129–133.
13. **Drost, E. M., et al.** 2005. Oxidative stress and airway inflammation in severe exacerbations of COPD. Thorax **60:**293–300.
14. **Fischer, B. M., and J. A. Voynow.** 2002. Neutrophil elastase induces MUC5AC gene expression in airway epithelium via a pathway involving reactive oxygen species. Am. J. Respir. Cell Mol. Biol. **26:**447–452.
15. **Guarner, J., and R. Falcón-Escobedo.** 2009. Comparison of the pathology caused by H1N1, H5N1, and H3N2 influenza viruses. Arch. Med. Res. **40:**655–661.
16. **Iizuka, T., et al.** 2005. Nrf2-deficient mice are highly susceptible to cigarette smoke-induced emphysema. Genes Cells **10:**1113–1125.
17. **Ishii, Y., et al.** 2005. Transcription factor Nrf2 plays a pivotal role in protection against elastase-induced pulmonary inflammation and emphysema. J. Immunol. **175:**6968–6975.
18. **Itoh, K., et al.** 1997. An Nrf2/small Maf heterodimer mediates the induction of phase II detoxifying enzyme genes through antioxidant response elements. Biochem. Biophys. Res. Commun. **236:**313–322.
19. **Kawai, T., and S. Akira.** 2007. Antiviral signaling through pattern recognition receptors. J. Biochem. **141:**137–145.
20. **Kawai, T., and S. Akira.** 2008. Toll-like receptor and RIG-I-like receptor signaling. Ann. N. Y. Acad. Sci. **1143:**1–20.
21. **Kikuchi, N., et al.** 2010. Nrf2 protects against pulmonary fibrosis by regulating the lung oxidant level and Th1/Th2 balance. Respir. Res. **11:**31.
22. **Kong, X., R. Thimmulappa, P. Kombairaju, and S. Biswal.** 2010. NADPH oxidase-dependent reactive oxygen species mediate amplified TLR4 signaling and sepsis-induced mortality in Nrf2-deficient mice. J. Immunol. **185:**569–577.
23. **Malhotra, D., et al.** 2008. Decline in NRF2-regulated antioxidants in chronic obstructive pulmonary disease lungs due to loss of its positive regulator, DJ-1. Am. J. Respir. Crit. Care Med. **178:**592–604.
24. **Mallia, P., and S. L. Johnston.** 2007. Influenza infection and COPD. Int. J. Chron. Obstruct. Pulmon. Dis. **2:**55–64.
25. **Molls, R. R., et al.** 2006. Keratinocyte-derived chemokine is an early biomarker of ischemic acute kidney injury. Am. J. Physiol. Renal Physiol. **290:**F1187–F1193.
26. **Pantano, C., N. L. Reynaert, A. van der Vliet, and Y. M. Janssen-Heininger.** 2006. Redox-sensitive kinases of the nuclear factor-kappaB signaling pathway. Antioxid. Redox Signal. **8:**1791–1806.
27. **Peterhans, E., M. Grob, T. Bürge, and R. Zanoni.** 1987. Virus-induced formation of reactive oxygen intermediates in phagocytic cells. Free Radic. Res. Commun. **3:**39–46.
28. **Rangasamy, T., et al.** 2004. Genetic ablation of Nrf2 enhances susceptibility to cigarette smoke-induced emphysema in mice. J. Clin. Invest. **114:**1248–1259.
29. **Reddy, N. M., et al.** 2009. Disruption of Nrf2 impairs the resolution of hyperoxia-induced acute lung injury and inflammation in mice. J. Immunol. **182:**7264–7271.
30. **Rudd, B. D., E. Burstein, C. S. Duckett, X. Li, and N. W. Lukacs.** 2005. Differential role for TLR3 in respiratory syncytial virus-induced chemokine expression. J. Virol. **79:**3350–3357.
31. **Song, K. S., et al.** 2003. Interleukin-1 beta and tumor necrosis factor-alpha induce MUC5AC overexpression through a mechanism involving ERK/p38 mitogen-activated protein kinases-MSK1-CREB activation in human airway epithelial cells. J. Biol. Chem. **278:**23243–23250.
32. **Suzuki, M., et al.** 2008. Down-regulated NF-E2-related factor 2 in pulmonary macrophages of aged smokers and patients with chronic obstructive pulmonary disease. Am. J. Respir. Cell Mol. Biol. **39:**673–682.
33. **Szulakowski, P., et al.** 2006. The effect of smoking on the transcriptional regulation of lung inflammation in patients with chronic obstructive pulmonary disease. Am. J. Respir. Crit. Care Med. **174:**41–50.
34. **Takeyama, K., et al.** 1999. Epidermal growth factor system regulates mucin production in airways. Proc. Natl. Acad. Sci. U. S. A. **96:**3081–3086.
35. **Thimmulappa, R. K., et al.** 2006. Nrf2 is a critical regulator of the innate immune response and survival during experimental sepsis. J. Clin. Invest. **116:**984–995.
36. **Voelkel, N. F., and R. Tuder.** 2000. COPD exacerbation. Chest **117**(Suppl. 2)**:**376S–379S.
37. **Wedzicha, J. A.** 2002. Exacerbations: etiology and pathophysiologic mechanisms. Chest **121**(Suppl.)**:**136S–141S.
38. **Wedzicha, J. A., and T. A. Seemungal.** 2007. COPD exacerbations: defining their cause and prevention. Lancet **370:**786–796.
39. **Wong, J. P., et al.** 2009. Activation of Toll-like receptor signaling pathway for protection against influenza virus infection. Vaccine **27:**3481–3483.
40. **Yang, S. R., et al.** 2006. Cigarette smoke induces proinflammatory cytokine release by activation of NF-kappaB and posttranslational modifications of histone deacetylase in macrophages. Am. J. Physiol. Lung Cell. Mol. Physiol. **291:**L46–L57.
41. **Yao, H., et al.** 2008. Genetic ablation of NADPH oxidase enhances susceptibility to cigarette smoke-induced lung inflammation and emphysema in mice. Am. J. Pathol. **172:**1222–1237.
42. **Zhu, Z., W. Tang, J. M. Gwaltney, Jr., W. Wu, and J. A. Elias.** 1997. Rhinovirus stimulation of interleukin-8 in vivo and in vitro: role of NF-κB. Am. J. Physiol. Lung Cell. Mol. Physiol. **273:**L814–L824.